Supplemental Data

S1. Table: Statistics from the structure determination process.

Protein Database entry:	1YQ3	1YQ4	9ZZZ
Inhibitor co-crystallized:	OAA	3-NP	Carboxin
A. DATA REDUCTION			
Space Group	$P2_12_12_1$	$P2_12_12_1$	$P2_1$
Unit Cell Dimensions	70.0 × 84.4 × 289.5 Å	69.6 × 83.5 × 288.6 Å	122.0 ×203.4 ×69.0; 90.0 90.0 90.0
Solvent content	64.6 %	63.9 %	64.6 %
V_M	3.47	3.40	3.47
X-ray wavelength [a]:	0.979462	1.0000, 0.97395	0.9800
Unique Reflections	79236	78612	166966
Resolution Range, Å [a] :	38 - 2.19 (2.27 - 2.19)	57. - 2.20 (2.24 - 2.20)	99-2.1 (2.14-2.10)
"Optical Resolution" [b]	1.72 Å	1.75 Å	1.66
Completeness :	87.5% (49%)	89.3% (56 %)	86.4
Data Redundancy:	4.5	2.7	4.5
R Merge on I :	0.119 (0.29)	0.116 (0.48)	0.19 (0.52)
$\langle I/\sigma_I \rangle$	11.9 (2.6)	11.8 (2.4)	18.5
B. REFINEMENT:			
Resolution	38.7 - 2.20 (2.24-2.19)	56.4 - 2.33 (2.33 - 2.38)	34.9 - 2.10 (2.1-2.15)
Data Cutoff (σ_F)	0.0	0.0	0.0
Completeness	89.2% (47.1%)	93.9% (80.2%)	86.0 (42.8)
# Reflections	78719 (2623)	68501 (3672)	166872 (5572)
R Value	0.176 (0.27)	0.205 (0.32)	0.195 (0.30)
Free R Value	0.225 (0.31)	0.259 (0.38)	0.235 (0.36)
Number Of Atoms Used			
Protein Atoms	8511	8511	16992
Heterogen Atoms	272	244	422
Solvent Atoms	942	611	1980
B Values			
From Wilson Plot	34.4 $Å^2$	30.9 $Å^2$	11.9 $Å^2$
Mean atomic B Value	47.8 $Å^2$	47.1 $Å^2$	31.3 $Å^2$
Anisotropic B_{11}, B_{22}, B_{33}	2.7, 15.7, -18.4 $Å^2$	2.8, 10.9, -13.7 $Å^2$	-2.8, 6.6, -3.8 $Å^2$
ESD,- (cross-validated)[c]			
From Luzzati Plot[c]	0.22 Å(0.31 Å)	0.28 Å (0.37 Å)	0.24, (0.30 Å)
From Sigmaa[c]	0.23 Å (0.11 Å)	0.32 Å (0.43 Å)	0.28, (0.34 Å)
Rms Deviations From Ideality			
Bond Lengths	0.022 Å	0.019 Å	0.032
Bond Angles	1.8°	1.9°	2.0°
Dihedral Angles	22.4°	22.3°	22.8
Improper Angles	1.02°	1.08°	1.15
C. VALIDATION:			
Residues in "Most Favored" region of Ramachandran	88.5%	87.3% 88.3	
Residues in Ramachandran "disallowed" region	0.3%	0.3%	0.1
Bad Contacts/100 residues	1.0	1.9	0.2
Overall G-factor (ProCheck):	0.0	0.2	0.3

[a]Statistics in the highest resolution shell are given in parentheses.
[b]Optical resolution is defined in reference (50).
[c]Cross-validated estimates of ESD are given in parentheses.

S2. Table. The detected ions by fragmenting 3-NP modified peptide DLASR*DVVSR using LTQ linear ion trap tandem mass spectrometry

	b (*m/z*)			y (*m*/z)					a (*m/z*)		
	normal	3-NP adduct	Decarboxylated 3-NP adduct	normal	3-NP adduct		Decarboxylated 3-NP adduct		Normal	3-NP adduct	Decarboxylated 3-NP adduct
	+ (DHI)	+ (DHI)	+ (DHI)	+ (DHI)	+ (DHI)	++ (DHI)	+ (DHI)	++ (DHI)	+	+	+
2	**229.5**	ND	ND	**262.6** (244..5)	ND	ND	ND	ND	**210.5**	ND	ND
3	**300.5** (282.5)	ND	ND	**361.6** (343.7)	ND	ND	ND	ND	272.6	ND	ND
4	**387.6** (369.6)	ND	ND	**460.7** (442.8)	ND	ND	ND	ND	359.6	ND	ND
5	ND	**626.4** (608.5)	ND (564.6)	**575.7** (557.7)	ND	ND	ND	ND	ND	ND	ND
6	ND	**741.4** (723.4)	**697.5** (679.5)	ND	**814.5** (796.4)	ND	**770.6** (752.6)	ND	ND	ND	ND
7	ND	**840.5** (822.4)	**796.4** (778.6)	ND	**901.4** (883.4)	**451.8** (433.9)	**857.6** (839.7)	**430.0**	ND	812.4	768.5
8	ND	**939.4** (921.4)	**895.5** (877.5)	ND	**972.4** (954.6)	**487.3** (478.1)	**928.5** (910.5)	**465.4** (456.6)	ND	911.5	867.5
9	ND	**1026.5** (1008.4)	**982.3** (964.5)	ND	ND	**543.8**	ND	**521.7** (512.7)	ND	998.5	954.6

+: Singly charged ion; ++: Doubly charged ion; DHI: Dehydrated ion; ND: not detected.
Bold: labeled in Figure 5.

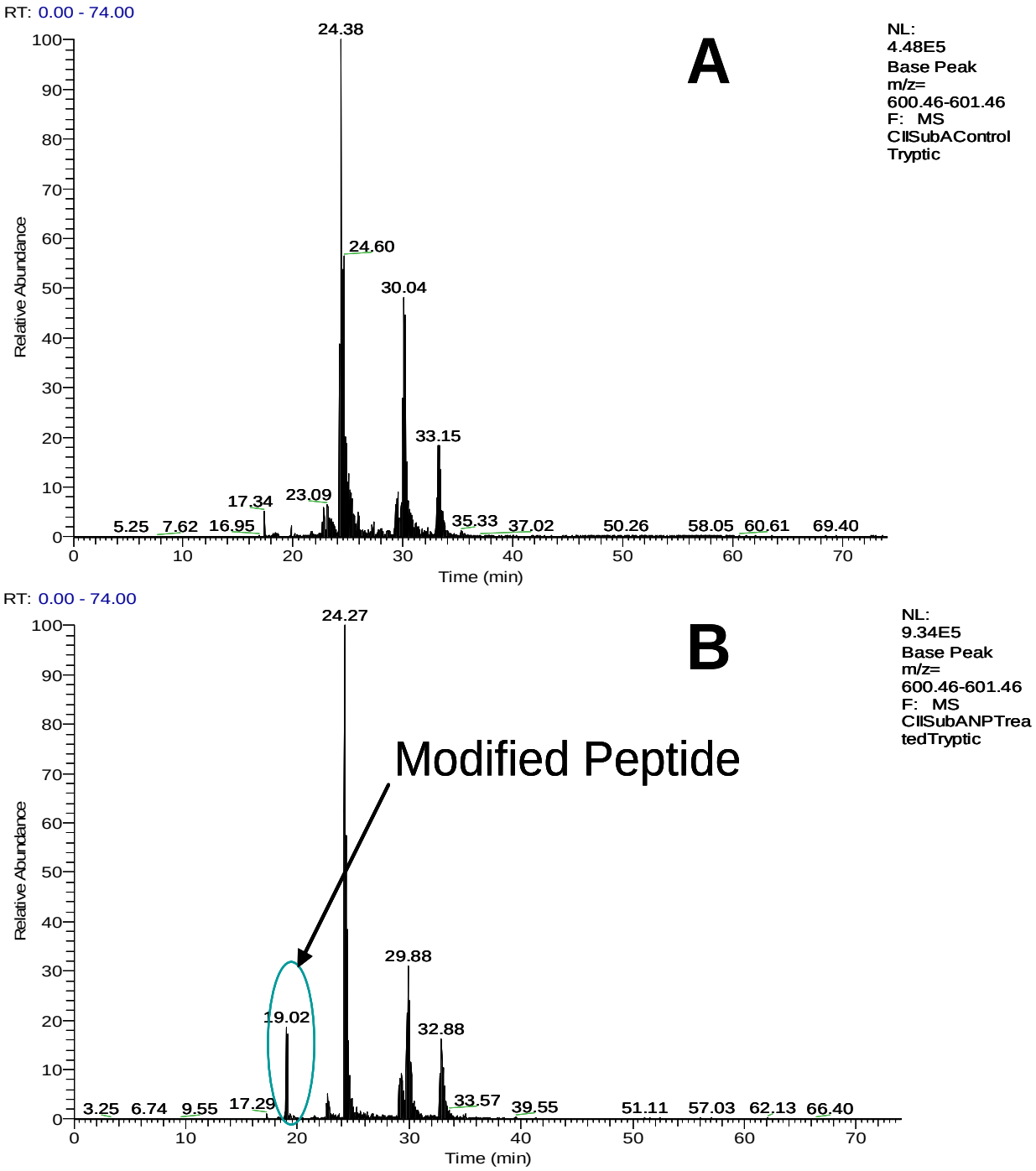

Figure S3. Selected ion chromatograms of *m/z* 600.9 obtained by reverse phase HPLC of the tryptic peptides of subunit A of the mitochondrial respiratory chain complex II from chicken heart monitored with a Finnigan LTQ linear ion trap tandem mass spectrometer. (A): the control sample; (B): the 3-NP inactivated complex II sample. Reaction conditions were given in Methods. The peak at 19.02 min in Figure B and absent in Figure A represents the doubly charged ion of the 3-NP modified peptide DLASR*DVVSR, as determined by analysis of the tandem mass spectrum.

S4-6. Simulated annealing omit maps of critical features. To guard against model bias, critical features were omitted from the model used to calculate the phases for the maps demonstrating those features. After omission of the indicated residues another round of refinement (consisting of simulated anealing from 1000 K in steps of 25 K, followed by 100 steps of conjugate gradient minimization) was carried out before calculating the map. The maps are expressed in terms of absolute electron density above the mean value for the cell. The structure factors were put on an approximate absolute scale based on the assumed cell contents using the CCP4 (32) program "truncate". Simulated annealing and map calculations were carried out with CNS (35) using coefficients (mF_o-DF_c), where m and D are weighting factors from the sigmaA treatment. Note that with these coefficients, residues which are correctly modeled and were *not* omitted have little density, due to cancellation of the nearly equal F_o and F_c contributions.

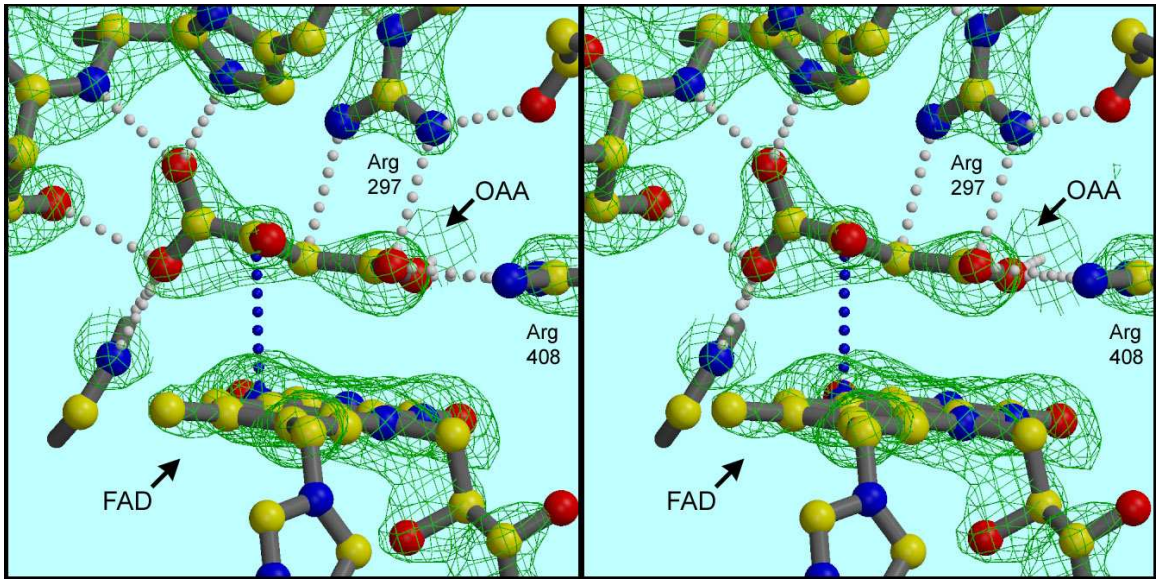

S4. Simulated annealing omit map of the ligand in structure 9zzz. The orientation is the same as that in Figure 2, but the map is a sigma-A-weighted difference map calculated with phases and F_c from the model after omitting the ligand and all atoms within 3.5 A of it. The map is contoured at 0.55 $e^-/Å^3$ above mean density.

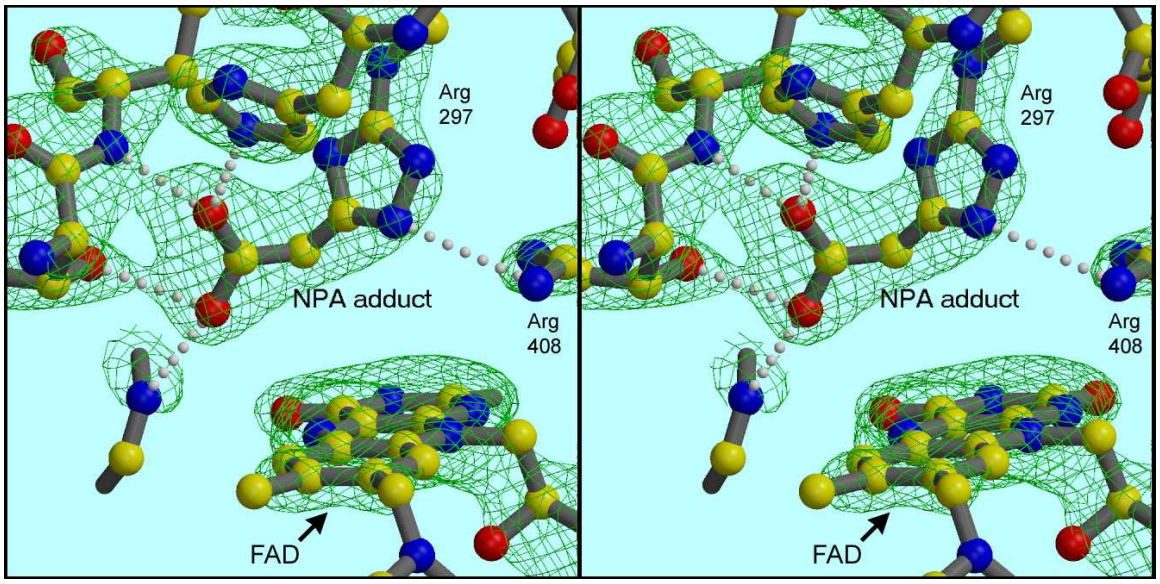

S5. Simulated annealing omit map of the 3-NP-modified Arg297 in structure 1YQ4. The orientation is the same as that in Figure 3, but the map is a sigma-A-weighted difference map calculated with phases and F_c from the model after omitting the Arg297, the ligand, and all residues within 3.5 A of them. The map is contoured at 0.45 $e^-/Å^3$ above mean density.

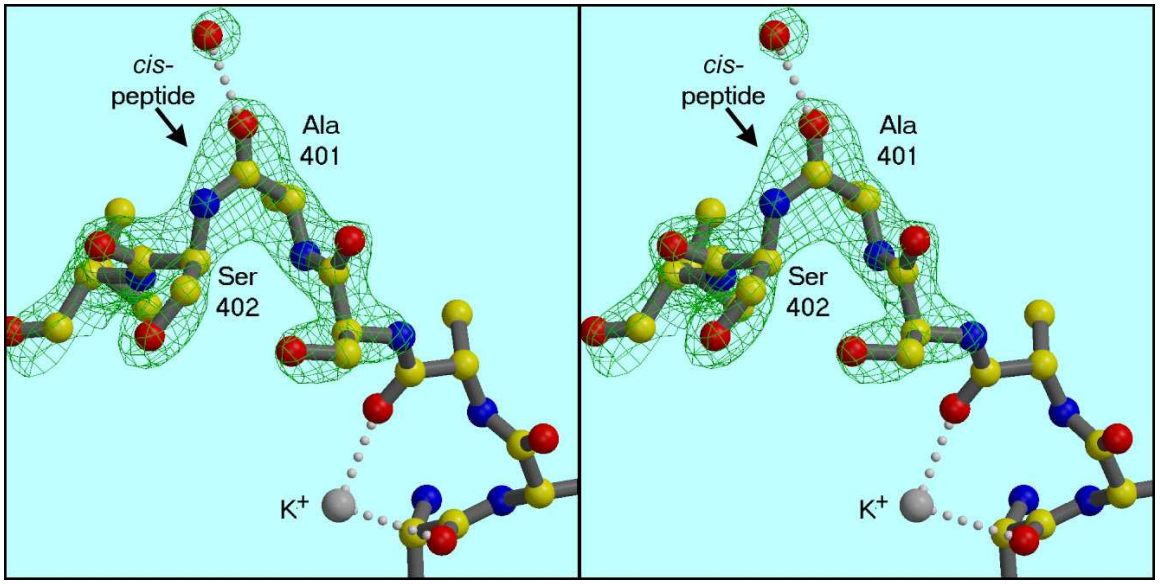

S6. Simulated annealing omit map of flavoprotein residues 401 - 402 in structure 1YQ3, demonstrating the *cis*-peptide bond. The map is a sigma-A-weighted difference map calculated with phases and F_c from the model after omitting the two residues and all atoms within 3.5 A of them. The map is contoured at 0.45 $e^-/Å^3$ above mean density.

S7. Evaluation of apparent differences between the avian and porcine structures.

Although the relation between the CAP and FAD domains in the *E. coli* and porcine SQR structures (1NTK and 1ZOY) is essentially the same "closed" conformation seen in the chicken SQR and *Shewanella* FCc structures, the catalytic arginine corresponding to Arg297 is modeled in a different rotamer which does not permit interaction with occupants of the site. Experimental x-ray data were deposited supporting the porcine structure, allowing us to test alternate conformations for this residue. After remodeling Arg 298 in rotamer 1 (like Arg297 in the chicken structure) and refining, the average atomic B-factor for the guanidino group decreased to 90 $Å^2$ as compared to 105 $Å^2$ in the deposited structure. The side chain of this remodeled residue was well covered by $2F_o$-F_c density contoured at 0.7σ. No density appeared in the place of the ligand except two peaks which may represent water molecules, supporting the authors' conclusion that the site is empty. Thus we believe that the catalytic arginine in the porcine structure is in the same position as that in the chicken, and the H-bonds to the ligand are not required to maintain this conformation.

Remodeling Arg298 of 1ZP0 in rotamer 1 put the guanidino in part of the density attributed to 3-NP. The remaining density accomodated the covalent adduct of 3-NP as modeled in the chicken structure 1YQ4. B-factors for the guanidino group decreased from about 150 in 1ZP0 to around 100 $Å^2$ after remodeling, however B-factors for 3NP increased from around 50 to 100 $Å^2$ after remodeling. We attribute the low B-factor of 3-NP in 1ZP0 to anti-correlation between occupancy and B-factor as refinement parameters at low resolution, and the fact that the 3-NPA was being used to fit the density of the guandino group as well.

The porcine structures 1ZOY and 1ZP0 were modeled with a *trans* peptide bond between residues Ala402 and Ser403 (corresponding to Ala401 and Ser402 in the chicken sequence). Because the authors deposited the raw data on which the structure was based, it was possible to test the conformations of the chicken model for compatibility with the porcine (1ZOY) dataset, and it was found that a *cis* peptide fit significantly better (Average B-factor for residue 403 of 48 $Å^2$, vs 60 $Å^2$ in the deposited structure). In 1ZOY, residue A402 is flagged as having the largest angular deviation in the structure (bond angle 96.4° for N-CA-C, deviation -14.8°), which became more normal (109.5) after refining with the cis-peptide.

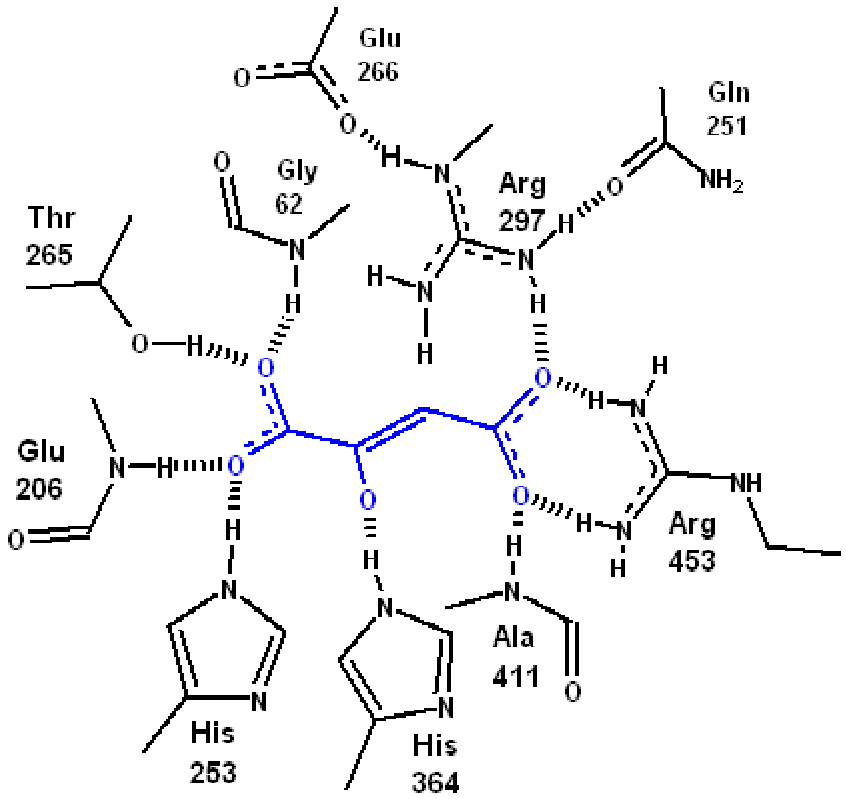

S8. Figure depicting the *enol* form of OAA as the "malate-like intermediate" in the dicarboxylate site. Another possibility is shown in Ref. (38), Figure 4b.